

NUMERICAL STUDY ON BIOLOGICAL TISSUE FREEZING USING DUAL PHASE LAG BIO-HEAT EQUATION

Dr. Sushil Kumar



*Department of Applied Mathematics and Humanities,
S. V. National Institute of Technology, Surat, India
E-mail: sushilk@amhd.svnit.ac.in*

- Introduction
- Mathematical Model
- Numerical Method
- Result and Discussion
- Conclusion
- Bibliography

- The heat transfer problems involving melting and freezing process are known as **phase change problems** and the phase change interface boundary movement depends on the absorption or liberation of latent heat.
- The heat transfer involved in phase change is necessary in biomedical applications such as cryopreservation and cryosurgery.

Cryosurgery

- It is a technique to treat tumour and can be used inside the body and on the skin.

Cryosurgery

- It is a technique to treat tumour and can be used inside the body and on the skin.
- The extreme cold is used for freezing and destroying abnormal cells by introducing liquid nitrogen through cryoprobe into the targeted region.

Cryosurgery

- It is a technique to treat tumour and can be used inside the body and on the skin.
- The extreme cold is used for freezing and destroying abnormal cells by introducing liquid nitrogen through cryoprobe into the targeted region.
- Also referred as cryotherapy or cryoablation.

Cryosurgery

- It is a technique to treat tumour and can be used inside the body and on the skin.
- The extreme cold is used for freezing and destroying abnormal cells by introducing liquid nitrogen through cryoprobe into the targeted region.
- Also referred as cryotherapy or cryoablation.
- It is used for the destruction of a large variety of tumors e.g. liver, prostate, bone tumors, vaginal tumors, skin cancer and hemorrhoids etc.

Cryosurgery

- It is a technique to treat tumour and can be used inside the body and on the skin.
- The extreme cold is used for freezing and destroying abnormal cells by introducing liquid nitrogen through cryoprobe into the targeted region.
- Also referred as cryotherapy or cryoablation.
- It is used for the destruction of a large variety of tumors e.g. liver, prostate, bone tumors, vaginal tumors, skin cancer and hemorrhoids etc.
- Freezing is induced using a cryoprobe made of specific metal, the tip of which is used to generate low temperature area around the diseased tissue region.

Introduction..



Cryosurgery is conducted by means of a cryoprobe either by placing its continuously cooled tip on or into the tissue to be frozen.



- Critical to cryosurgery success is **maximizing freezing damage within a confined target region**, while **minimizing cooling injury to its surrounding tissues**.

- Critical to cryosurgery success is **maximizing freezing damage within a confined target region**, while **minimizing cooling injury to its surrounding tissues**.
- However, it is still difficult to monitor the temperature inside tumor non-invasively and accurately during the treatment, which results in uncertainty in the final outcome of the procedure and the inability to ensure complete destruction of the entire target tumor.

- Critical to cryosurgery success is **maximizing freezing damage within a confined target region**, while **minimizing cooling injury to its surrounding tissues**.
- However, it is still difficult to monitor the temperature inside tumor non-invasively and accurately during the treatment, which results in uncertainty in the final outcome of the procedure and the inability to ensure complete destruction of the entire target tumor.
- This is because the survival of the tumor cells is largely dependent on the lowest end temperature that they experience

- Critical to cryosurgery success is **maximizing freezing damage within a confined target region**, while **minimizing cooling injury to its surrounding tissues**.
- However, it is still difficult to monitor the temperature inside tumor non-invasively and accurately during the treatment, which results in uncertainty in the final outcome of the procedure and the inability to ensure complete destruction of the entire target tumor.
- This is because the survival of the tumor cells is largely dependent on the lowest end temperature that they experience
- As a result, **precise and detailed information of the temperature field** that develops in tumor during the freezing process is essential to the surgeon for judging tumor destruction.

- Critical to cryosurgery success is **maximizing freezing damage within a confined target region**, while **minimizing cooling injury to its surrounding tissues**.
- However, it is still difficult to monitor the temperature inside tumor non-invasively and accurately during the treatment, which results in uncertainty in the final outcome of the procedure and the inability to ensure complete destruction of the entire target tumor.
- This is because the survival of the tumor cells is largely dependent on the lowest end temperature that they experience
- As a result, **precise and detailed information of the temperature field** that develops in tumor during the freezing process is essential to the surgeon for judging tumor destruction.
- Such information may be obtained by mathematical modeling during pre-treatment planning to guide the surgeon.

- Various models have been proposed to model the heat transport phenomena in blood perfuse tissues e.g. Pennes Model[3], The Chen and Holmes (CH) Model[4], The Weinbaum, Jiji and Lemons (WJL) Model[5, 6], The Wainbaum and Jiji (WJ) Model[7].
- **Pennes bio-heat equation** [3] is the most widely applied model for temperature distribution in the living biological tissues.

$$\rho c \frac{\partial T}{\partial t} = -\nabla \cdot \mathbf{q} + (\rho c)_b w_b (T_b - T) + Q_m, \quad (1)$$

where ρ is density of tissue; k , thermal conductivity; c_b , specific heat of blood; w_b , blood perfusion rate; T , temperature; t , time; T_b , arterial blood temperature and Q_m is the metabolic heat generation in the tissue.

- In Pennes bioheat equation, the heat conduction in biological tissue is modeled by using Fourier's law

$$\mathbf{q}(t, X) = -k\nabla T(t, X) \quad (2)$$

where \mathbf{q} and $T(t, X)$ represent heat flux and temperature at position $X = (x, y, z)$ and time t respectively.

- It assumes that \mathbf{q} and ∇T appear at the same time instant. This implies that thermal signals propagate with an infinite speed[8].

- In Pennes bioheat equation, the heat conduction in biological tissue is modeled by using Fourier's law

$$\mathbf{q}(t, \mathbf{X}) = -k\nabla T(t, \mathbf{X}) \quad (2)$$

where \mathbf{q} and $T(t, \mathbf{X})$ represent heat flux and temperature at position $\mathbf{X} = (x, y, z)$ and time t respectively.

- It assumes that \mathbf{q} and ∇T appear at the same time instant. This implies that thermal signals propagate with an infinite speed[8].
- In fact, heat is always found to propagate at finite speed.

- In Pennes bioheat equation, the heat conduction in biological tissue is modeled by using Fourier's law

$$\mathbf{q}(t, X) = -k\nabla T(t, X) \quad (2)$$

where \mathbf{q} and $T(t, X)$ represent heat flux and temperature at position $X = (x, y, z)$ and time t respectively.

- It assumes that \mathbf{q} and ∇T appear at the same time instant. This implies that thermal signals propagate with an infinite speed[8].
- In fact, heat is always found to propagate at finite speed.
- On the other hand, biological systems are non-homogeneous where heat flux responds to temperature gradient via relaxation behaviour.

- To solve the paradox occurred in Pennes model different other models were developed. **Cattaneo[9]** and **Vernotte[10]** independently proposed a modified heat flux model as

$$\mathbf{q}(t + \tau_q, X) = -k\nabla T(t, X), \quad (3)$$

where, τ_q is delay between the heat flux vector and the temperature gradient.

- In eq. (3), the **temperature gradient is established at time t** , but the heat flux vector will be established at a later time $t + \tau_q$, at the same point X .
- Using equation (3), one can get the following hyperbolic bioheat equation

$$\tau_q \rho c \frac{\partial^2 T}{\partial t^2} + (\rho c + \tau_q \rho_b c_b w_b) \frac{\partial T}{\partial t} = k \nabla^2 T(t, X) + Q_m + \rho_b c_b w_b (T_b - T) \quad (4)$$

This equation is called **thermal wave model of bioheat equation**, as it predicts a wave like behavior of heat transport.

- Many researchers have studied the heat transfer in tissue using thermal wave bioheat model. Singh and Kumar[11, 12] studied heat transfer during cryosurgery using hyperbolic model.

$$\tau_q \rho c \frac{\partial^2 T}{\partial t^2} + (\rho c + \tau_q \rho_b c_b w_b) \frac{\partial T}{\partial t} = k \nabla^2 T(t, X) + Q_m + \rho_b c_b w_b (T_b - T) \quad (4)$$

This equation is called **thermal wave model of bioheat equation**, as it predicts a wave like behavior of heat transport.

- Many researchers have studied the heat transfer in tissue using thermal wave bioheat model. Singh and Kumar[11, 12] studied heat transfer during cryosurgery using hyperbolic model.
- Although a lot of experiments confirmed that CV constitutive relation produces a more accurate prediction than the classical Fourier law, it still establishes an instantaneous response between the temperature gradient and the energy transport [13, 14, 15].

- It also establishes that the temperature gradient is always the cause for heat flux while heat flux is always effect in the process of energy transport [13, 14].

- It also establishes that the temperature gradient is always the cause for heat flux while heat flux is always effect in the process of energy transport [13, 14].
- Further thermal wave model does not consider the micro-scale response in space, although it considers the micro scale response in time [14, 16, 17].

- It also establishes that the temperature gradient is always the cause for heat flux while heat flux is always effect in the process of energy transport [13, 14].
- Further thermal wave model does not consider the micro-scale response in space, although it considers the micro scale response in time [14, 16, 17].
- In-depth study presents that the CV constitutive relation describes only the fast transient effects and not the micro-structural interactions.

- It also establishes that the temperature gradient is always the cause for heat flux while heat flux is always effect in the process of energy transport [13, 14].
- Further thermal wave model does not consider the micro-scale response in space, although it considers the micro scale response in time [14, 16, 17].
- In-depth study presents that the CV constitutive relation describes only the fast transient effects and not the micro-structural interactions.
- In order to solve the paradox in Fourier model and to consider the effect of micro structural effect in the fast transient process of heat transport, **Tzou[14]** proposed a dual phase lag (DPL) model that allows either the temperature gradient to precede heat flux vector or the heat flux vector to precede the temperature gradient i.e.

$$\mathbf{q}(t + \tau_q, X) = -k\nabla T(t + \tau_T, X). \quad (5)$$

Equation (5), represents that the temperature gradient at a point X of the material at time $t + \tau_T$ corresponds to the heat flux density vector at time $t + \tau_q$ at the same point X .

- The delay time τ_T is interpreted as being caused by the micro structural interactions and is called the phase-lag of the temperature gradient[13, 14].
- The other delay time, τ_q is interpreted as the relaxation time due to the fast-transient effects of thermal inertia and is called the phase-lag of the heat flux. Both of the phase-lags are treated as intrinsic thermal or structural properties of the material.

The first order Taylor's expansion of the Eq. (5) gives the dual phase lag constitutive relation.

$$\mathbf{q} + \tau_q \frac{\partial \mathbf{q}}{\partial t} = -k \nabla \left\{ T(t, X) + \tau_T \frac{\partial T}{\partial t} \right\}. \quad (6)$$

Elimination of \mathbf{q} from energy balance equation (Eq. 1) and the dual phase lag constitutive relation (Eq. 6) leads to the following equation

$$\tau_q \rho c \frac{\partial^2 T}{\partial t^2} + (\rho c + \tau_q \rho_b c_b w_b) \frac{\partial T}{\partial t} = k \nabla^2 \left\{ T(t, X) + \tau_T \frac{\partial T}{\partial t} \right\} + Q_m + \rho_b c_b w_b (T_b - T) \quad (7)$$

Equation (7) is the modification of the Pennes bio-heat equation by considering non-Fourier effect and is called as dual-phase lag bio-heat equation.

- It converts into **hyperbolic** bio heat equation if $\tau_T = 0$, and into **parabolic** bio heat equation for $\tau_T = 0$ and $\tau_q = 0$.
- Many researchers[18, 19, 20, 21, 22, 23] have studied the dual-phase lag bio-heat model without phase change. Liu *et al.*[18, 19] explain the dual-phase lag bio-heat model during hyperthermia treatment. Majchrzak[20] has described the solution of the dual-phase lag bio-heat model by using the boundary element method. Zhang *et al.*[23] have studied the dual-phase lag model with non-equilibrium heat transfer in arterial blood, venous blood and biological tissue and also calculated the phase lag of temperature gradient and heat flux in different condition. Zhou *et al.*[24, 25] have considered the dual-phase lag bio-heat model during the laser heating of living tissues. Singh and Kumar[26] have also studied dual phase change heat transfer model in three layer skin tissue.

- In present study, the dual-phase lag model is obtained by modifying the classical Pennes bio-heat equation.

- In present study, the dual-phase lag model is obtained by modifying the classical Pennes bio-heat equation.
- non-ideal property, blood perfusion and metabolic heat generation have been considered for studying the effect of parameters in the freezing of biological tissue during phase change.

- In present study, the dual-phase lag model is obtained by modifying the classical Pennes bio-heat equation.
- non-ideal property, blood perfusion and metabolic heat generation have been considered for studying the effect of parameters in the freezing of biological tissue during phase change.
- The effects of both phase lags and blood perfusion on temperature profile and interface positions have been studied.

- In present study, the dual-phase lag model is obtained by modifying the classical Pennes bio-heat equation.
- non-ideal property, blood perfusion and metabolic heat generation have been considered for studying the effect of parameters in the freezing of biological tissue during phase change.
- The effects of both phase lags and blood perfusion on temperature profile and interface positions have been studied.
- Comparative study of three heat transfer models *i.e.* parabolic, hyperbolic and DPL has also been presented here.

Governing Equations

One dimensional dual-phase lag bio-heat equation in frozen region and unfrozen region are given below.

(a) In frozen region: for $0 \leq x \leq s(t)$

$$\tau_q \rho_f c_f \frac{\partial^2 T_f}{\partial t^2} + \rho_f c_f \frac{\partial T_f}{\partial t} = k_f \frac{\partial^2 T_f}{\partial x^2} + \tau_T k_f \frac{\partial^3 T_f}{\partial t \partial x^2}. \quad (8)$$

Governing Equations

One dimensional dual-phase lag bio-heat equation in frozen region and unfrozen region are given below.

(a) In frozen region: for $0 \leq x \leq s(t)$

$$\tau_q \rho_f c_f \frac{\partial^2 T_f}{\partial t^2} + \rho_f c_f \frac{\partial T_f}{\partial t} = k_f \frac{\partial^2 T_f}{\partial x^2} + \tau_T k_f \frac{\partial^3 T_f}{\partial t \partial x^2}. \quad (8)$$

(b) In unfrozen region: for $s(t) \leq x \leq l$

$$\tau_q \rho_u c_u \frac{\partial^2 T_u}{\partial t^2} + (\rho_u c_u + \tau_q \rho_b c_b w_b) \frac{\partial T_u}{\partial t} = k_u \left(\frac{\partial^2 T_u}{\partial x^2} + \tau_T \frac{\partial^3 T_u}{\partial t \partial x^2} \right) + Q_m + \rho_b c_b w_b (T_b - T_u) \quad (9)$$

(c) Conditions at phase change interface $x = s(t)$ are

$$\rho_f L \frac{\partial s}{\partial t} + \tau_q \rho_f L \frac{\partial^2 s}{\partial t^2} = k_f \left(\frac{\partial T_f}{\partial x} + \tau_T \frac{\partial^2 T_f}{\partial t \partial x} \right) - k_u \left(\frac{\partial T_u}{\partial x} + \tau_T \frac{\partial^2 T_u}{\partial t \partial x} \right), \quad (10)$$

and

$$T_u(t, s(t)) = T_f(t, s(t)) = T_{ph}, \quad (11)$$

where, subscripts f , u , and ph denote frozen, unfrozen and phase change respectively and l denotes the length of tissue.

Major difficulty, that arise in phase change heat transfer of biological tissue is its non-linearity due to variable disconnection between different phase region and unknown position of phase change interfaces.

Thus, for the solution purpose we consider the enthalpy formulation of dual-phase lag bio-heat equation for phase change problem associated with freezing.

Using enthalpy $H(T) = \int_{T_0}^T c dT$, where T_0 is reference temperature, Eqs.

(8)-(11) reduce in single equation as follows

$$\tau_q \rho \frac{\partial^2 H}{\partial t^2} + \left(\rho + \frac{\tau_q \rho_b c_b w_b}{c} \right) \frac{\partial H}{\partial t} = k \left(\frac{\partial^2 T}{\partial x^2} + \tau_T \frac{\partial^3 T}{\partial t \partial x^2} \right) + Q_m + \rho_b c_b w_b (T_b - T), \quad (12)$$

Enthalpy and tissue temperature are related as[39, 40]

$$H = \begin{cases} c_f(T - T_{ms}), & T < T_{ms} \\ c_a(T - T_{ms}) + \frac{L}{\Delta T}(T - T_{ms}), & T_{ms} \leq T \leq T_{ml} \\ L + c_a\Delta T + c_u(T - T_{ml}), & T > T_{ml}, \end{cases} \quad (13)$$

where, L is latent heat of freezing, $c_a = \frac{c_f + c_u}{2}$ and $\Delta T = T_{ml} - T_{ms}$.

Assumptions:

Following assumptions have been made to solve the dual phase lag bio-heat transfer model

- (i) Heat conduction follows non-Fourier law of heat conduction.
- (ii) Latent heat is constant.
- (iii) Heat source due to metabolism and blood perfusion is present when tissue is not frozen [28, 29].
- (iv) Non-ideal property of tissue is used with liquidus and solidus temperature as -1°C and -8°C respectively [41, 42].
- (v) Thermo-physical properties are different in frozen and unfrozen region.
- (vi) One-dimensional model has been considered.

Initial and Boundary Conditions:

Followings initial and boundary conditions are used for the mathematical model

(a) at $t = 0$

$$T_i(x, t) = T_0 = 37^{\circ}\text{C} \quad \text{and} \quad \frac{\partial T_i}{\partial t} = 0, \quad i = u, f \quad (14)$$

(b) at $x = 0$

$$T_i(x, t) = T_c, \quad i = u, f \quad (15)$$

(c) at $x = l$

$$\frac{\partial T_i(x, t)}{\partial x} = 0, \quad i = u, f, \quad (16)$$

where, T_0 is body core temperature, 37°C and T_c is cryoprobe temperature, -196°C

- In biological tissues, phase change occurs over a wide range and there exist moving boundaries between the two phases thus resulting mathematical models are non-linear.
- Analytical solutions are only possible for one dimensional, steady state cases[27]. Numerical methods appear to offer a more practical approach for solving these problems.
- Existing numerical approaches can be divided into two categories: **front tracking and non front tracking**[27]. **Enthalpy** method, a non front tracking method is easy to implement as fixed grids can be used for computation purpose and the non-linearity at the moving boundary can also be avoided.
- FDMs are the most popular choice for numerical solution of phase change problems [11, 12, 28, 29, 30, 31, 32, 33, 34, 35] though FEM,[36, 37, 38] boundary element methods [29] have also been introduced for the phase change problem in biological tissue.

The space length l is divided into N equal parts where

$$N = \frac{l}{\Delta x}; \quad x_i = i\Delta x \quad \text{and} \quad t_n = n\Delta t,$$

where i and n are space and time indexes respectively;
 Δx and Δt are the increment in space and time respectively.

Introducing forward difference approximation for first order time derivative and central difference approximation for space derivative and second order time derivative into the Eq. (12), we get

$$\begin{aligned}
 H_i^{n+1} = & H_i^n + \left\{ \frac{A_i^n}{A_i^n + B_i^n} \right\} (H_i^n - H_i^{n-1}) - \left\{ \frac{2E_i^n + 2D_i^n + F_i^n}{A_i^n + B_i^n} \right\} T_i^n \\
 & + \left\{ \frac{E_i^n + D_i^n}{A_i^n + B_i^n} \right\} (T_{i+1}^n + T_{i-1}^n) - \left\{ \frac{D_i^n}{A_i^n + B_i^n} \right\} (T_{i+1}^{n-1} + T_{i-1}^{n-1} \\
 & - 2T_i^{n-1}) + \left\{ \frac{F_i^n}{A_i^n + B_i^n} \right\} T_b + \frac{Q_m}{A_i^n + B_i^n} \quad (17)
 \end{aligned}$$

where,

$$\begin{aligned}
 A_i^n &= \frac{\tau_q \rho_i^n}{(\Delta t)^2}, & B_i^n &= \left[\frac{\rho_i^n}{(\Delta t)} + \frac{\tau_q \rho_b c_b w_b}{c_i^n (\Delta t)} \right], \\
 D_i^n &= \frac{k_i^n \tau_T}{(\Delta t)(\Delta x)^2}, & E_i^n &= \frac{k_i^n}{(\Delta x)^2}, & F_i^n &= \rho_b c_b w_b.
 \end{aligned}$$

The above Eq. (17) can be written as

$$\begin{aligned} H_i^{n+1} &= (1 + U_i^n) H_i^n - U_i^n H_i^{n-1} - (2W_i^n + 2V_i^n + Y_i^n) T_i^n \\ &\quad + (W_i^n + V_i^n) (T_{i+1}^n + T_{i-1}^n) \\ &\quad - V_i^n (T_{i+1}^{n-1} - 2T_i^{n-1} + T_{i-1}^{n-1}) + Y_i^n T_b + Z_i^n \end{aligned} \quad (18)$$

where,

$$\begin{aligned} U_i^n &= \frac{A_i^n}{A_i^n + B_i^n}, & V_i^n &= \frac{D_i^n}{A_i^n + B_i^n}, & W_i^n &= \frac{E_i^n}{A_i^n + B_i^n}, \\ Y_i^n &= \frac{F_i^n}{A_i^n + B_i^n}, & Z_i^n &= \frac{Q_m}{A_i^n + B_i^n}. \end{aligned}$$

Equation (18), gives the enthalpy at $(n+1)^{th}$ time step in terms of enthalpy and temperature at n^{th} time level. The time and space increments are adjusted in such a way that they should satisfy the stability criteria,

$$\max \frac{(\Delta t) \{2k(\Delta t) + 2k_{\tau T} + \rho_b c_b w_b (\Delta t) (\Delta x)^2\}}{(\Delta x)^2 \{2c_{\tau q} \rho + c \rho (\Delta t) + \tau_q \rho_b c_b w_b (\Delta t)\}} \leq 1. \quad (19)$$

After getting the enthalpy at $(n+1)^{th}$ time level, temperature at $(n+1)^{th}$ time level can be obtained by reverting Eq. 13 as follows

$$T = \begin{cases} \frac{H}{c_f} + T_{ms}, & H < 0, \\ \frac{H \Delta T}{c_a \Delta T + L} + T_{ms}, & 0 \leq H \leq L + c_a \Delta T, \\ \frac{H - L - c_a \Delta T}{c_u} + T_{ml}, & H > L + c_a \Delta T. \end{cases} \quad (20)$$

Thermal properties of tissue

Parameter	Value
Density of unfrozen tissue(kg/m^3)	1000
Specific heat of unfrozen tissue($J/kg^{\circ}C$)	3600
Thermal conductivity of unfrozen tissue($W/m^{\circ}C$)	0.5
Density of frozen tissue(kg/m^3)	1000
Specific heat of frozen tissue($J/kg^{\circ}C$)	1800
Thermal conductivity of frozen tissue($W/m^{\circ}C$)	2
Density of blood(kg/m^3)	1050
Specific heat of blood ($J/kg^{\circ}C$)	3770
Blood perfusion in tissue ($ml/s/ml$)	0.005
Metabolic heat generation (W/m^3)	4200
Latent heat (J/m^3)	250000
The upper limit of phase change temperature($^{\circ}C$)	-1
The lower limit of phase change temperature($^{\circ}C$)	-8
Arterial blood temperature ($^{\circ}C$)	37

Results and Discussion

- In present study, the numerical results are shown for dual phase lag, hyperbolic ($\tau_T = 0$) and parabolic ($\tau_T = 0, \tau_q = 0$) bio-heat transfer with phase change during freezing of biological process.

Results and Discussion

- In present study, the numerical results are shown for dual phase lag, hyperbolic ($\tau_T = 0$) and parabolic ($\tau_T = 0, \tau_q = 0$) bio-heat transfer with phase change during freezing of biological process.
- For the numerical solution, the value of the phase-lag of the heat flux are $\tau_q = 0s, \tau_q = 5s, \tau_q = 10s, \tau_q = 15s$ and the value of the phase-lag of the temperature gradient are $\tau_T = 0s, \tau_T = 5s, \tau_T = 10s$ [20, 44, 45, 46].

Results and Discussion

- In present study, the numerical results are shown for dual phase lag, hyperbolic ($\tau_T = 0$) and parabolic ($\tau_T = 0, \tau_q = 0$) bio-heat transfer with phase change during freezing of biological process.
- For the numerical solution, the value of the phase-lag of the heat flux are $\tau_q = 0s, \tau_q = 5s, \tau_q = 10s, \tau_q = 15s$ and the value of the phase-lag of the temperature gradient are $\tau_T = 0s, \tau_T = 5s, \tau_T = 10s$ [20, 44, 45, 46].
- During the freezing process of the biological tissue, the **temperature distribution** and **interface position** are important for the prediction of the damage of the infected tissues and minimum damage of the healthy tissues.

Results and Discussion...

- ✓ The temperature distributions in the tissue at time $t = 600s$ with respect to distance x for the DPL, hyperbolic and parabolic models are shown in Fig. 1.
- ✓ It is observed that **parabolic model gives lowest temperature** in the tissue with comparison to DPL and hyperbolic model, while, The **highest temperature is obtained for hyperbolic model**.
- ✓ This shows that parabolic model gives fastest heat flow in the media while slowest is for hyperbolic model.

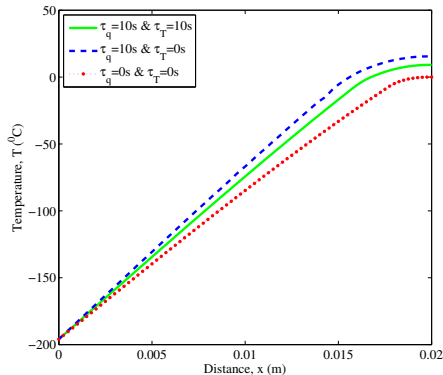


Figure 1: The temperature profile along the target tissue for parabolic, hyperbolic and DPL model at the time $t = 600s$.

Results and Discussion...

To study the effect of these three models on temperature distribution with respect to time in tissue, the variation of temperature versus time for parabolic, hyperbolic and DPL model at the point $x = 0.01m$ is plotted in Fig. 2.

Again from Fig. 2, it is clear that decline in temperature is highest for parabolic and lowest for hyperbolic with comparison to DPL model.

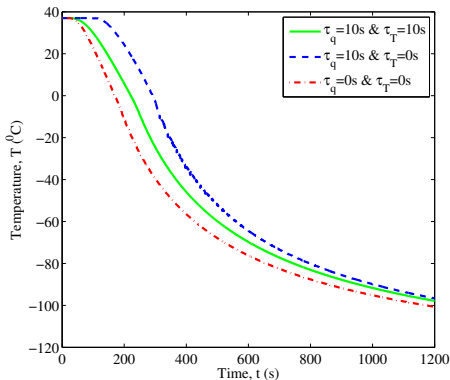


Figure 2: The variation of temperature versus time for parabolic, hyperbolic and DPL model at the point $x = 0.01m$.

The **liquidus and solidus** interfaces position of the phase change interface during the freezing process for DPL, parabolic and hyperbolic models are shown in Fig. 3 and Fig. 4 respectively.

Results and Discussion...

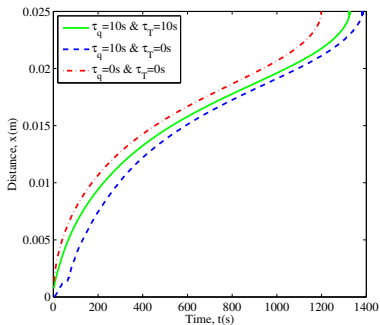


Figure 3: Liquidus Interface position for parabolic, hyperbolic and DPL model.

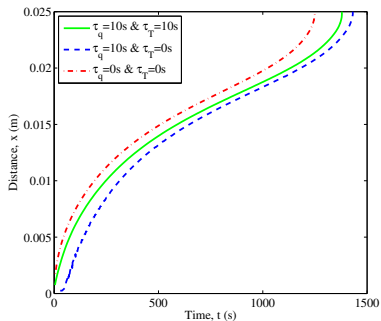


Figure 4: Solidus Interface position for parabolic, hyperbolic and DPL model.

It is clear that the phase change interfaces movement is slowest for the hyperbolic model while fastest is for parabolic model i.e., the time required for complete tissue freezing is **minimum for parabolic** model while it is **maximum for hyperbolic** model.

Effect of τ_q :

To study the effect of phase lag on freezing process, temperature profiles in tissue at time $t = 800s$ are plotted in Fig. 5 for different value of τ_q , i.e. 5s, 10s, 15s keeping fixed value of $\tau_T = 5s$.

In this case, lowest temperature is observed for minimum value of τ_q .

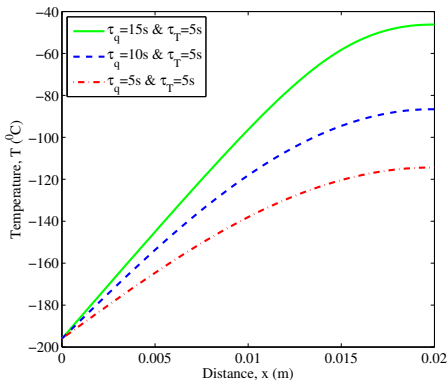


Figure 5: The temperature profile along the target tissue for DPL model at the time $t = 800s$

The liquidus and solidus interface position for

$$\tau_q = 15s; \quad \tau_q = 10s \quad \tau_q = 5s \text{ and } \tau_T = 5s$$

are plotted in Fig. 6 and Fig. 7 respectively.

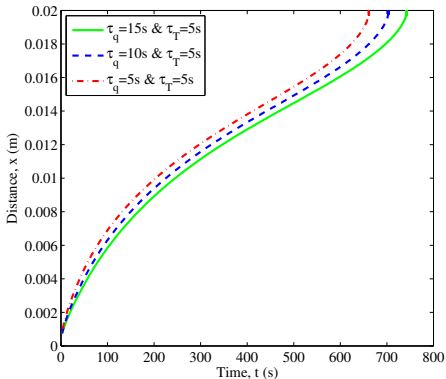


Figure 6: Liquidus Interface position for DPL model

Time taken to reach the liquidus interface at $x = 0.02m$ is 742s, 703s and 661s for $\tau_q = 15s$, $\tau_q = 10s$ and $\tau_q = 5s$ respectively

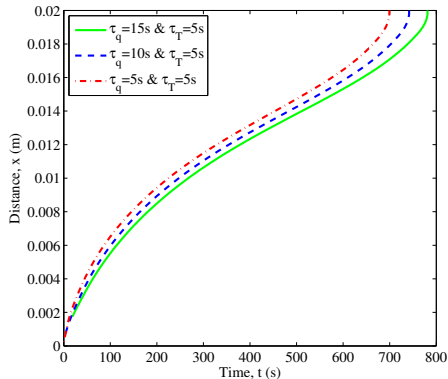


Figure 7: Solidus Interface position for DPL model

while solidus interface reaches at $x = 0.02m$ in time is 781.32s, 741.63s and 699.33s for $\tau_q = 15s$, $\tau_q = 10s$ and $\tau_q = 5s$ respectively.

- ✓ It shows that the phase change interfaces for the DPL model move slower with increasing value of τ_q .

- ✓ It shows that the phase change interfaces for the DPL model move slower with increasing value of τ_q .
- ✓ That is the time required for complete tissue freezing in the DPL model for fixed value of the phase-lag of the temperature gradient $\tau_T = 5s$ increases with increased value of τ_q .

- ✓ It shows that the phase change interfaces for the DPL model move slower with increasing value of τ_q .
- ✓ That is the time required for complete tissue freezing in the DPL model for fixed value of the phase-lag of the temperature gradient $\tau_T = 5s$ increases with increased value of τ_q .
- ✓ τ_q denote the delay time due to the fast transient effect of thermal inertias, thus a larger value of τ_q will result delay in tissue freezing.

Effect of Blood Perfusion:

In the freezing process, energy transfer in the biological tissue is due to

- thermal conduction
- blood tissue convection
- blood perfusion, and
- metabolic heat generation

These parameters have significant effect of transient temperature profile and position of solidus and liquidus interfaces.

The effect of blood perfusion on freezing process using DPL, hyperbolic and parabolic model has been studied in present study.

(a). DPL model:

For DPL model position of liquidus and solidus interfaces for

$$w_b = 0.05 \text{ ml/s/ml}, \quad w_b = 0.01 \text{ ml/s/ml} \quad \text{and} \quad w_b = 0.005 \text{ ml/s/ml}$$

are plotted in Fig. 8 and Fig. 9 respectively.

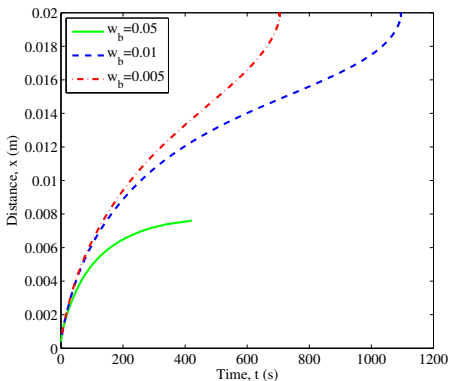


Figure 8: Liquidus Interface position for DPL model at $\tau_q = 10s$ and $\tau_T = 10s$ for different value of blood perfusion

The liquidus interface reaches at distance $x = 0.02m$ in time $t = 1095s$ and $t = 705s$ for $w_b = 0.01ml/s/ml$ and $w_b = 0.005ml/s/ml$ respectively.

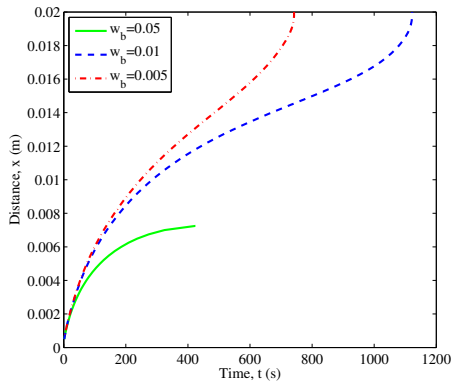


Figure 9: Solidus Interface position for DPL model at $\tau_q = 10s$ and $\tau_T = 10s$ for different value of blood perfusion

Similarly solidus interface reaches at distance $x = 0.02m$ in time $t = 1122.4s$ and $t = 742s$ for $w_b = 0.01ml/s/ml$ and $w_b = 0.005ml/s/ml$ respectively.

(b).Hyperbolic model:

For hyperbolic model position of liquidus and solidus interfaces for $w_b = 0.05 \text{ ml/s/ml}$, $w_b = 0.01 \text{ ml/s/ml}$ and $w_b = 0.005 \text{ ml/s/ml}$ are plotted in Fig. 10 and Fig. 11 respectively.

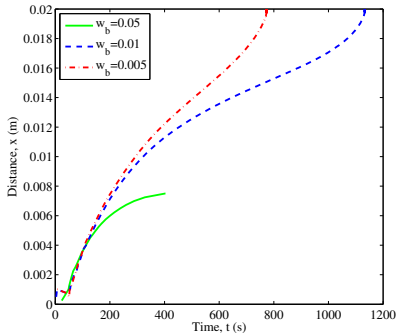


Figure 10: Liquidus Interface position for hyperbolic model at $\tau_q = 10s$ and $\tau_T = 0s$ for different value of blood perfusion

The liquidus interface reaches at distance $x = 0.02m$ in time $t = 1132s$ and $t = 773.15s$ for $w_b = 0.01ml/s/ml$ and $w_b = 0.005ml/s/ml$ respectively.

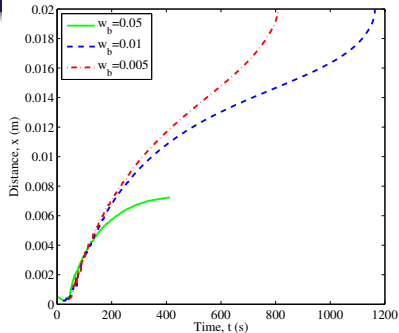


Figure 11: Solidus Interface position for hyperbolic model at $\tau_q = 10s$ and $\tau_T = 0s$ for different value of blood perfusion

Similarly solidus interface reaches at distance $x = 0.02m$ in time $t = 1163.2s$ and $t = 807.67s$ for $w_b = 0.01ml/s/ml$ and $w_b = 0.005ml/s/ml$ respectively.

(c). Parabolic Model:

For parabolic model position of liquidus and solidus interfaces for $w_b = 0.05 \text{ ml/s/ml}$, $w_b = 0.01 \text{ ml/s/ml}$ and $w_b = 0.005 \text{ ml/s/ml}$ are plotted in Fig. 12 and Fig. 13 respectively.

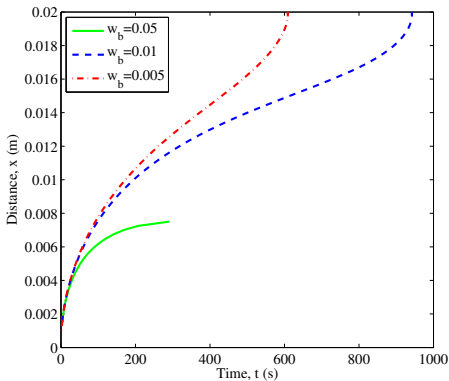


Figure 12: Liquidus Interface position for parabolic model at $\tau_q = 0s$ and $\tau_T = 0s$ for different value of blood perfusion

The liquidus interface reaches at distance $x = 0.02m$ in time $t = 942.30s$ and $t = 609.15s$ for $w_b = 0.01ml/s/ml$ and $w_b = 0.005ml/s/ml$ respectively.

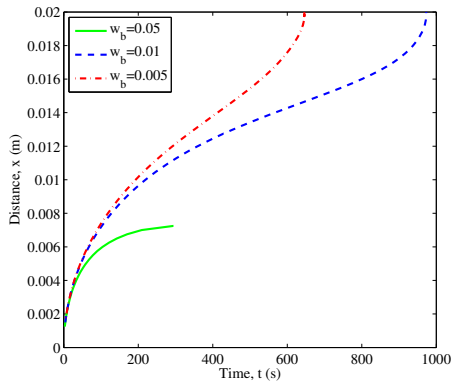


Figure 13: Solidus Interface position for parabolic model at $\tau_q = 0s$ and $\tau_T = 0s$ for different value of blood perfusion










Similarly solidus interface reaches at distance $x = 0.02m$ in time $t = 973s$ and $t = 645.94s$ for $w_b = 0.01ml/s/ml$ and $w_b = 0.005ml/s/ml$ respectively.

It is observed that for increased value of blood perfusion freezing process slows down.

Due to blood perfusion, heat is added to the tissue which opposes the freezing process and hence slows it down.











- In present study, the temperature dependent enthalpy formulation and finite difference method is used to obtain the temperature profile and interface position based on DPL model.
- Comparison of DPL model with parabolic and hyperbolic model of heat transport is also made in the study.
- It is observed, that among the DPL, hyperbolic and parabolic model total time required for complete tissue freezing is least for parabolic model and largest for hyperbolic model while for DPL model it is moderate.
- The phase lag of heat flux and the phase lag of temperature gradient have a significant effect on the temperature profile and interface position of phase change interfaces
- In DPL model, the phase change interface accelerates with decreasing value of phase lag of heat flux.

Bibliography

-  J.C. Bischof, J. Bastack , B. Rubinsky, *ASME J. Biomech. Eng.*, **114**, 467 (1992).
-  K.J. Chua, S.K. Chou, J.C. Ho, *Journal of Biomechanics*, **40**, 100, (2007).
-  H.H. Pennes, *J. Applied physiology*, **1**, 93, (1948).
-  M.M. Chen, K.R. Holmes, *Annals of the New York Academy of sciences*, **335**, 137, (1980).
-  L.M. Jiji, S. Weinbaum, D.E. Lemons, *ASME J. Biomechanical Engineering*, **106**, 331, (1984).
-  S. Weinbaum, L.M. Jiji, D.E. Lemons, *ASME J. Biomechanical Engineering*, **106**, 321, (1984).
-  S. Weinbaum, L.M. Jiji, *ASME J. Biomechanical Engineering*, **107**, 131, (1985).
-  L. Wang, J. Fan, *ASME J. of heat transfer*, **133**, 011010-1, (2011).
-  C. Cattaneo, *Comptes Rendus de l'Académie des Sciences*, **247**, 431, (1958).

-  P. Vernotte, *Comptes Rendus de l'Académie des Sciences*, **246**, 3154, (1958).
-  S. Singh, S. Kumar, *Mathematical Modelling and Analysis*, **20:4**, 443, (2015).
-  S. Singh, S. Kumar, *Journal of Mechanics in Medicine in Biology*, DOI: 10.1142/S0219519416500172, online ready.
-  D.Y. Tzou, *ASME J. Heat Transfer*, **117**, 8, (1995).
-  D.Y. Tzou, *Macro-to Microscale Heat Transfer: The Lagging Behavior*, Taylor and Francis, Washington, DC (1997).
-  L.Q. Wang, *Int. J. Heat Mass Transfer*, **37**, 2627, (1994).
-  D.Y. Tzou, M.N. Ozisik, R.J. Chiffelle, *J. Heat Transfer*, **116**, 1034, (1994).
-  M.N. Ozisik, D.Y. Tzou, *ASME J. Heat Transfer*, **116**, 526, (1994).
-  K.C. Liu, H. Chen, *International Journal of Heat and mass transfer*, **52**, 1185, (2009).

-  K.C. Liu, H. Chen, *International Journal of Thermal Sciences*, **49**, 1138, (2010).
-  E. Majchrzak, *Computer Modeling in Engineering and Sciences*, **69(1)**, 43 (2010).
-  E. Majchrzak, T. Lukasz, *19th International Conference on Computer Methods in Mechanics CMM*, 337, (2011).
-  N. Afrin , N. Y. Zhang , J. K. Chen, *International Journal of Heat and mass transfer*, **54**, 2419 (2011).
-  Y. Zhang, *International Journal of Heat and mass transfer*, **52**, 4829, (2009).
-  J. Zhou, J.K. Chen, Y. Zhang, *Computers in Biology and Medicine*, **39**, 286, (2009).
-  J. Zhou, Y. Zhang, J.K. Chen, *International Journal of Thermal Sciences*, **48**, 1477, (2009).
-  S.Singh, S. Kumar, *International Journal of Thermal Sciences*, **86**, 12, (2014).

-  J. Crank, Free and moving boundary problems, University Press, New York, 1984.
-  Z.S. Deng, J. Liu, *Numerical Heat Transfer: Part A*, **46**, 487 (2004).
-  Z.S. Deng, J. Liu, *Eng Anal Bound Elem*, **28(2)**, 97, (2004).
-  Y. Rabin, A. Shitzer, *J Biomech Eng.*, **120(1)**, 32, (1998).
-  S. Kumar, V.K. Katiyar, *Int. J. Appl. Math. Mech.*, **3(3)**,1, (2007).
-  R.I. Andrushkiw, *Mathematical and Computer Modelling*, **13**, 1, (1990).
-  M. Zerroukat, C.R. Chatwin, Computational moving boundary problem, John Wiley and Sons, New York, 1993.
-  J.C. Rewcastle, G.A. Sandison, K. Muldrew, J.C. Saliken, B.J. Donnelly, *Med. Phys.*, **28**, 1125, (2001).
-  S. Kumar, V.K. Katiyar, *Int. J Appl Mech.*, **2(3)**, 617, (2010).
-  G. Comini and D.S Giudice, *ASME J. Heat Transfer*, **98**, 543, (1976).

-  A. Weill, A. Shitzer, P.B. Yoseph, *Journal of Biomechanical Engineering*, **115**, 374, (1993).
-  J.Y. Zhang, G.A. Sadison, J.Y. Murthy and L.X. Xu, *Journal of Biomechanical Engineering*, **127**, 279, (2005).
-  C. Bonacina, G. Comini, *Int J heat mass transfer*, **16**, 1825 (1973) .
-  N.E. Hoffmann, J.C. Bischof, *ASME J. Biomech. Eng.*, **123**, 301, (2001).
-  Y. Rabin, A. Shitzer, *J. Heat Transfer*, **117**, 425, (1995).
-  Y. Rabin, A. Shitzer, *ASME J Heat Biomech Eng*, **119**, 146, (1997).
-  Z.S. Deng, J. Liu, *Journal of Thermal Stresses*, **26**, 779, (2003).
-  A. Moradi, H. Ahamdikia, *Journal of Engineering in Medicine*, **226(5)**, 406, (2012).
-  H. Ahamdikia, A. Moradi, R. Fazlali, B. Parsa, *J Mech Sci Technol*, **26(6)**, 1937 (2012).



L. Jing, C. Xu , L.X. Xu, *Biomedical Engineering, IEEE Transactions*, **46(4)**, 420, (1999).

Thanks